

SDC, Materials and Methods

Differentiation of CMs from human iPS

The human iPS (253G1) were purchased from the RIKEN (Tsukuba, Japan) and maintained as previously described ¹. Briefly, the cells were maintained in primate embryonic SC medium (ReproCELL, Yokohama, Japan) supplemented with 5 ng/mL basic fibroblast growth factor (bFGF; ReproCELL) on a feeder layer of mitomycin C-treated mouse embryonic fibroblasts (ReproCELL). The cells were passaged every three or four days using CKT solution (ReproCELL). The iPSs were differentiated into CMs in the bioreactor system. The iPS aggregates (approximately 2×10^7) from 10 culture dishes (100-mm diameter) were resuspended in 100 mL of mTeSR1 (Stemcell Technologies, Vancouver, BC, Canada) containing 10 μ M Y27632 (Wako Pure Chemical Industries, Osaka, Japan) and seeded into a 250-mL bioreactor (Bio Jr. 8; ABLE Co., Tokyo, Japan) equipped with a temperature sensor; pH electrodes; inoculation, harvest, and sample ports; and a two-bladed delta-like paddle for stirring. The dissolved oxygen content was monitored using a Fibox3 optical sensor (PreSens, Regensburg, Germany). The software for MiniJar8 100-mL bioreactor was used for data acquisition and process control. Aeration was performed by the headspace. The agitation rate was 40 rpm; dissolved oxygen was maintained at 40% with air, oxygen, or nitrogen; pH was maintained at 7.2 by CO₂ addition; and the temperature was maintained at 37°C during the entire process. After one day, the cells were cultured in mTeSR1 without Y27632, and the medium was exchanged every day until day 3. The embryoid bodies were cultured in the StemPro34 medium containing 50 μ g/mL ascorbic acid (Sigma-Aldrich, St. Louis, MO, USA), 2 mM L-glutamine, and 400 μ M 1-thioglycerol (Sigma-Aldrich). The following growth factors and small molecules were

added on the indicated days: days 3–4, 0.5 ng/mL bone morphogenetic protein (BMP) 4 (R&D Systems, Minneapolis, MN, USA); days 4–7, 10 ng/mL BMP4, 5 ng/mL bFGF, and 3 ng/mL activin A (R&D Systems); days 7–9, 4 μ M IWR-1 (Wako Pure Chemical Industries); and after day 9, 5 ng/mL VEGF (R&D Systems) and 10 ng/mL bFGF. The culture medium was replaced on days 4, 7, 9, 11, and 14.

Porcine MI model

The experiments were performed using female CLAWN miniature swine (weighing 18–25 kg, 6–10-months old; Kagoshima Miniature Swine Research Center, Kagoshima, Japan). The induction of experimental MI has been previously described². Briefly, the animals were preanesthetized by intramuscular injection of ketamine hydrochloride 20 mg/kg (Ketalar, Tokyo, Japan) and xylazine 2 mg/kg (Seractar, Bayer, Tokyo), placed in the supine position and intubated and ventilated with oxygen using a respirator. The anesthetic state was maintained by the inhalation of 2% isoflurane (Wako Pure Chemical Industries) and by continuous injection of 6 mg/kg/h propofol (Diprivan; AstraZeneca, Osaka, Japan). The body temperature, electrocardiogram (ECG), blood pressure, and pulse oximeter were monitored throughout the surgical procedure. A left thoracotomy was performed and the proximal root of the LAD branching from the left main trunk was exposed. To induce MI, a 2.5-mm ameroid constrictor (COR-2.5-SS; National Instruments, Austin, TX, USA) was placed on the proximal portion of coronary artery number 6. When ventricular fibrillation occurred, electrical defibrillation was immediately performed. If arrhythmia occurred when the chest was open, lidocaine (2 mg/kg intravenous [i.v.] bolus) was administered. The chest was sutured in layers and the animals were allowed to recover. Standard post-operative care

was administered according to the Animal Use Guidelines of the Osaka University. As the transplanted cells were derived from human cells, all the animals received a peri-operative injection of tacrolimus (50 mg i.v.) and were administered a triple-drug regimen of tacrolimus (1 mg/kg/day), MMF (500 mg/day), and corticosteroids (20 mg/day) with food. Myocardial infarction was induced in 60 pigs; 11 died of hemorrhage and ventricular fibrillation during the procedure, and three died of cardiac arrhythmia one month later. Another 16 pigs were excluded from the study as their echocardiograms showed an LVEF > 50% prior to cell transplantation. The remaining 29 animals were randomly assigned to the iPS-CM (n = 7), SM (n = 7), MSC (n = 7), and MI only (n = 8) groups.

Cell sheet transplantation

The cell sheet transplantation was performed as previously described² one month after LAD ligation. Immediately before transplantation, the cell sheets were detached from the temperature-responsive dish. The animals were anesthetized and the heart was exposed by median sternotomy. The infarct area was identified visually by surface scarring and abnormal wall motion. The cell sheets were transplanted onto the ischemic myocardium of pigs in the cell treatment groups; the sham animals were subjected to the surgical procedure without transplantation. To prevent dislocation of the sheets, the pericardium was closed before suturing the chest.

Cardiac MRI

To assess cardiac function, we performed 1.5 Tesla MRI (Signa EXCITE XI TwinSpeed 1.5T v.11.1; GE Healthcare). The animals were anesthetized with 2%

inhaled isoflurane and placed in the supine position within the scanner under ECG monitoring. The LVEF and thickening fraction were quantified from the short-axis images using the AZE VirtualPlace program (AZE, Tokyo, Japan). The cine imaging was performed with the following MR parameters: repetition time (TR) = 3.7 ms, echo time (TE) = 1.7 ms, flip angle = 45°, matrix size = 224 × 224, field of view = 30 cm × 30 cm, and slice thickness = 7 mm, with 20 phases acquired across the heartbeat cycle. The infarcted area was identified via delayed enhancement MRI (0.25 mL/kg gadodiamide hydrate bolus), which was performed with the following parameters: TR = 6.7 ms, TE = 3.2 ms, flip angle = 20°, matrix size = 256 × 192, field of view = 30 cm × 23 cm, and slice thickness = 7 mm.

Echocardiography

To evaluate regional myocardium function, the speckle-tracking analysis was performed with a commercially available system. Digital gray-scale two-dimensional cine loops from three consecutive heartbeats were obtained from long- and short-axis views. The mid-LV short-axis views were selected with the papillary muscle as a consistent internal anatomic landmark at depths of 11–20 cm. The frame rate was 44–49 Hz for gray-scale imaging. The sector depth was optimized to allow complete LV myocardial visualization while maximizing frame rate. Routine B-mode grey-scale images were analyzed for frame-by-frame myocardial movement by the speckle pattern matching technology. The transverse strain was assessed from the mid-level long-axis views. A region of interest was traced in the counterclockwise direction on the endocardium from the right-hand mitral annulus in the long-axis view by a point-and-click approach. A second large concentric circle was then automatically generated and manually adjusted

near the epicardium or was manually traced. The radial strain was assessed from the mid-LV short-axis view. A circular region of interest was traced in the counterclockwise direction on the endocardium beginning at 09:00 h at end-systole by the point-and-click approach. A second larger concentric circle was then automatically generated and manually adjusted near the epicardium or was manually traced. The mid-LV image was divided into six standard segments, and the time-strain curves were generated from each segment. Radial dyssynchrony was defined as a time difference between the anterior LV wall and posterior wall segmental peak strain ³. The speckle-tracking data were analyzed using an off-line software (Toshiba Medical Systems).

Hemodynamic parameters and wall stress

The hemodynamic parameters were measured via a catheter (3 mm outer diameter) inserted into the LV through the apical dimple. The wall stress was calculated based on wall thickening as determined by cardiac MRI and from hemodynamic data according to the following formula ⁴: systolic wall stress = LV systolic pressure × LV chamber radius / (2 × wall thickness).

Protocol of rest and cardiac work conditions in the PET scanning experiment

Following the intravenous administration of 200-300 MBq of ¹¹C acetate, the rest condition PET imaging data were acquired for 15 min. Pharmacological stress was induced using dobutamine. Following the rest condition data acquisition, dobutamine was administered with two stepwise increases in the infusion rate (10 µg/kg/min for 5 min and 20 µg/kg/min for 15 min). The second injection of ¹¹C acetate was initiated at

the end of the first step of dobutamine infusion, and the stress PET imaging data were acquired for 15 min thereafter ⁵.

Antibodies

The mouse monoclonal antibody (1:500) and rabbit polyclonal antibody (1:50) against CD31 were purchased from Abcam (Cambridge, UK). The mouse monoclonal antibody against SMA (Dako, Glostrup, Denmark; 1:50) and rabbit polyclonal antibody against α -sarcomeric actinin (Abcam; 1:50) were also used. The rabbit polyclonal antibody against cTnT, desmin, ssDNA, and CD90 was obtained from Abcam (1:100). The mouse monoclonal antibody against fMHC and CD105 were obtained from Abcam (1:100).

Flow cytometry analysis

For cTnT staining, the cells were fixed with BD CytotfixBD Cytotfix/Cytoperm solution for 30 min at 4°C followed by labeling with anti-cTnT antibody diluted in BD Perm/Wash buffer. For CD56 and CD105 labeling, the cells were incubated with the appropriate antibodies diluted in phosphate-buffered saline containing 2% fetal bovine serum. The cells were sorted on a FACS Canto II cytometer and analyzed with the BD FACS Diva software (both from BD Biosciences, Franklin Lakes, NJ, USA).

Vascular density and CM apoptosis

The LV was sectioned into three short-axis cross-sections from the base to the apex and each ring was sectioned into 12 blocks according to coronary anatomy. Each tissue specimen from the mid-LV ring was embedded in paraffin and cut into 5- μ m thick

sections. To visualize the vascular structures, the slides were immunolabeled with antibodies against CD31 and SMA. The microscopic images of labeled areas were randomly acquired. A total of five images per sample in the infarct area and two samples per animal were analyzed. The vascular (capillary) density is expressed as the number of CD31+ vessels and arteriolar density as the number of CD31+/SMA+ vessels per unit area (mm²). The sections were incubated with anti-cTnT antibody (1:200) to detect CMs. The myocardial samples were also incubated with the mouse monoclonal anti-ssDNA antibody (Abcam; 1:100) to identify apoptotic cells. The nuclei were stained with Hoechst 33342 (Dojindo Laboratories, Kumamoto, Japan; 1:100).

Supplemental data

Paracrine factors from cultured iPS-CM, SM and MSC

It has been shown that cell therapy to the heart produces paracrine effect, in which the transplanted cells release a variety of cardiac protective factors into the adjacent native cardiac tissue to enhance the native regenerative processes, such as angiogenic and antiapoptotic effects⁷. In the present study, the capacity to release cardiac protective factors, such as vascular endothelial growth factor (VEGF), stromal derived factor-1 (SDF-1), and insulin like growth factor-1 (IGF-1), in the culture supernatants of cell preparation was investigated in vitro. The analysis of conditioned medium from the iPS-CMs, SMs, and MSC cultures by enzyme-linked immunosorbent assay (R&D System, Minneapolis, MN, USA) revealed that the concentration of SDF-1, VEGF, and IGF-1 was not significantly different among the cell types (Supplement Figure 7). This indicates that the paracrine effect of the iPS-CMs therapy is expected for functional recovery, similar to that of the other somatic cell therapies.

Supplemental references

- [1] Matsuura K, Wada M, Shimizu T, et al. Creation of human cardiac cell sheets using pluripotent stem cells. *Biochem Biophys Res Commun.* 2012; 425: 321-327.
- [2] Miyagawa S, Saito A, Sakaguchi T, et al. Impaired myocardium regeneration with skeletal cell sheets—a preclinical trial for tissue-engineered regeneration therapy. *Transplantation.* 2010; 90: 364-371.
- [3] Tops LF, Suffoletto MS, Bleeker GB, et al. Speckle-tracking radial strain reveals left ventricular dyssynchrony in patients with permanent right ventricular pacing. *J Am Coll Cardiol.* 2007; 50: 1180-1188.
- [4] Moriarty TF. The law of Laplace. Its limitations as a relation for diastolic pressure, volume, or wall stress of the left ventricle. *Circ Res.* 1980; 46: 321-331.
- [5] Croteau E, Gascon S, Bentourkia M, et al. [11C]Acetate rest-stress protocol to assess myocardial perfusion and oxygen consumption reserve in a model of congestive heart failure in rats. *Nucl Med Biol.* 2012; 39: 287-294.
- [6] Fukushima S, Sawa Y, Suzuki K. Choice of cell-delivery route for successful cell transplantation therapy for the heart. *Future Cardiol.* 2013; 9: 215-227.

Supplemental figure

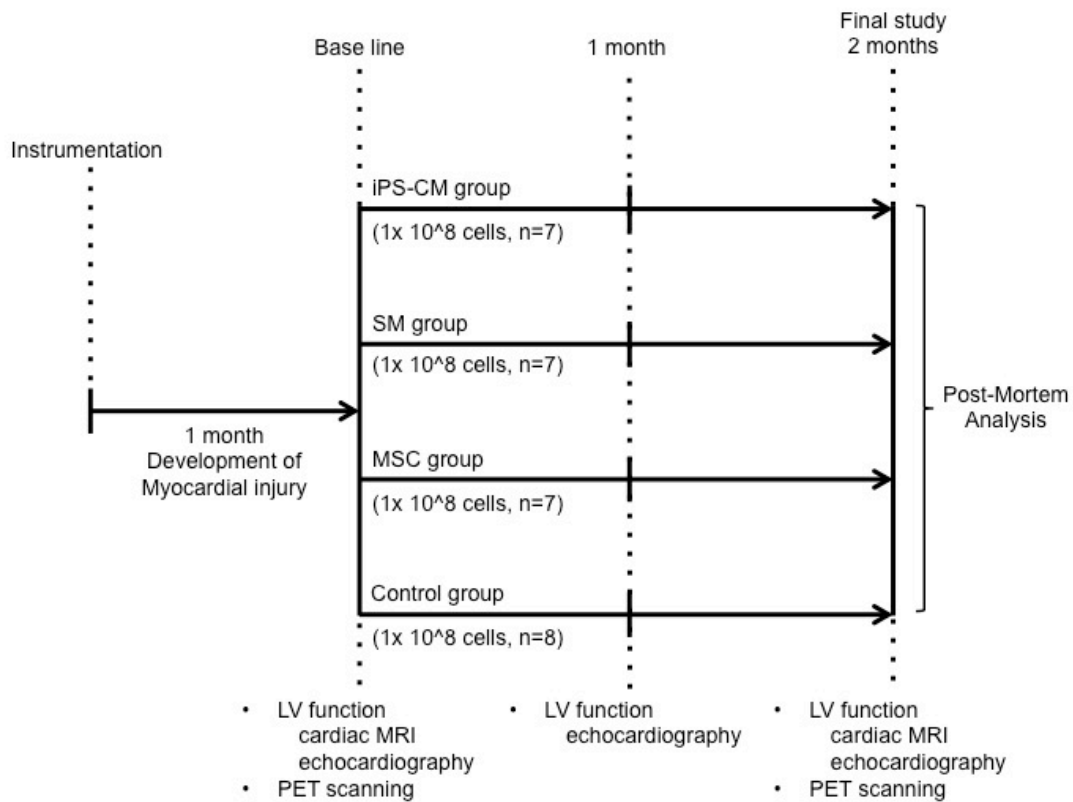


Figure S1. Experimental protocol. Chronic MI was induced in the pigs with an ameroid constrictor applied to the LAD and was established after one month, during which a baseline closed-chest analysis was carried out to assess the LV function (cardiac MRI, echocardiography, and PET scanning). The animals were then randomly assigned to one of the four experimental groups: iPS-CM (n = 7), SM (n = 7), MSC (n = 7), and control (n = 8). The effect of cell therapy was evaluated 1 month after cell transplantation by echocardiography. Follow-up studies were performed on all animals 2 months later, subsequently they were euthanized and their hearts were excised for post-mortem histopathological analysis.

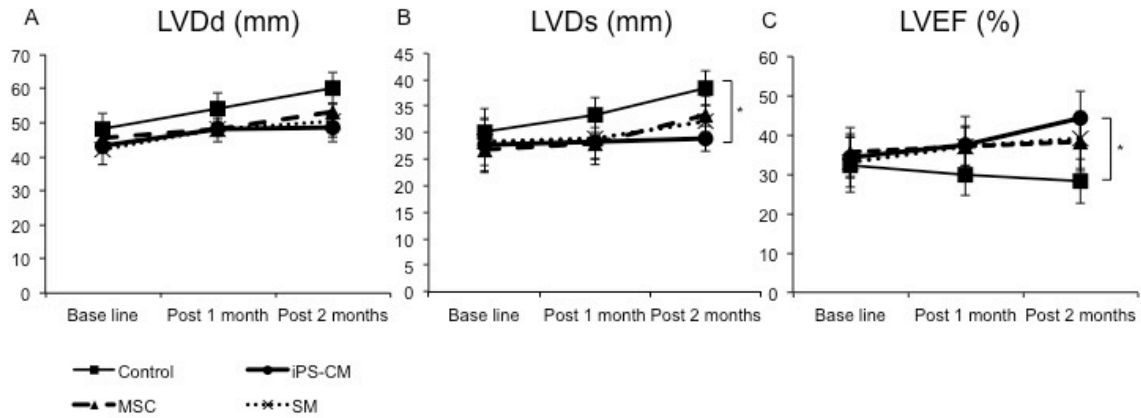


Figure S2. Myocardial infarction visualized by DHE MRI and regional definition. (A) The IZ was visualized by DHE MRI one month after MI (arrows). (B) Representative cross section of the whole heart two months after the operation (Masson's trichrome staining). (C) Definition of the IZ, BZ, and RZ. The IZ was marked as 30° sectors between the region enhanced by DHE; the BZ was defined as 30° sectors neighboring the infarcted segment; and the RZ comprised the remaining myocardium.

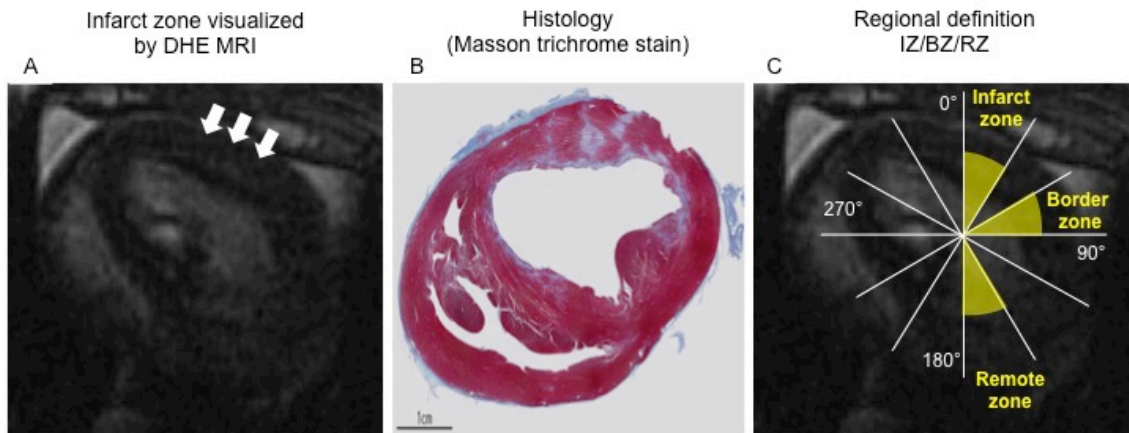


Figure S3. Protocol of rest and cardiac work conditions in the PET scanning experiment. Following the intravenous administration of 200–300 MBq of ^{11}C acetate, the rest condition PET imaging data were acquired for 15 min. The pharmacological stress was induced using dobutamine. Following the rest condition data acquisition, dobutamine was administered with two stepwise increases in the infusion rate (10 $\mu\text{g}/\text{kg}/\text{min}$ for 5 min and 20 $\mu\text{g}/\text{kg}/\text{min}$ for 15 min). The second injection of ^{11}C acetate was initiated at the end of the first step of dobutamine infusion, and the stress PET imaging data were acquired for 15 min thereafter.

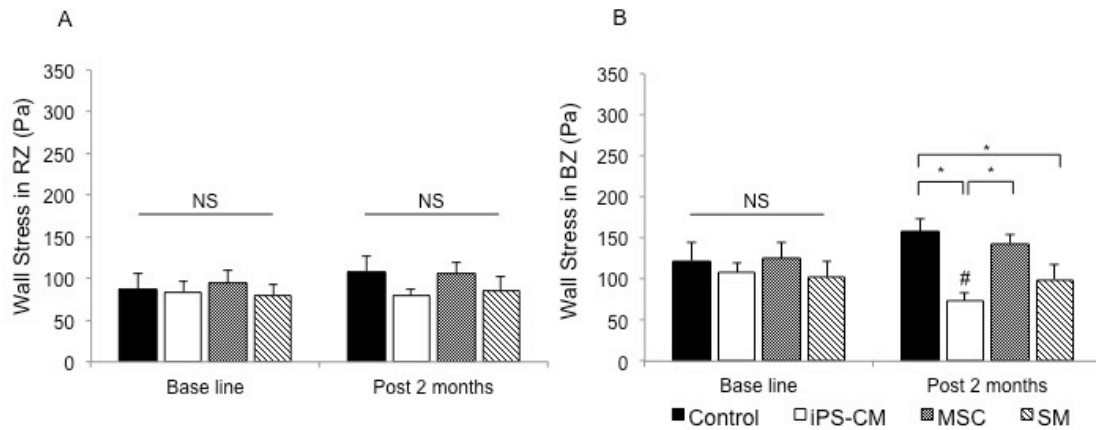


Figure S4. Effects of the transplanted iPS-CM, SM, and MSC sheets on global cardiac function assessed by echocardiography at baseline, one and two months after cell therapy. (A) Left ventricular diastolic diameter (LVDD); there was no differences in the baseline value among the groups. LVDD at one and two months after cell therapy gradually increased in all cell therapy and control groups relative to those values at the baseline. (B) Left ventricular systolic diameter (LVDs); the iPS-CM therapy inhibited the dilation of LVDs when compared with that of the control group (* $P < 0.05$). The other cell therapies also inhibited the dilation at one month after cell therapy, but not after that. (C) Left ventricular ejection fraction (LVEF); the iPS-CM therapy improved LVEF two months after cell therapy when compared with that of the other cell therapies. The control group showed a significant reduction in LVEF compared with that of the iPS-CM group (* $P < 0.05$).

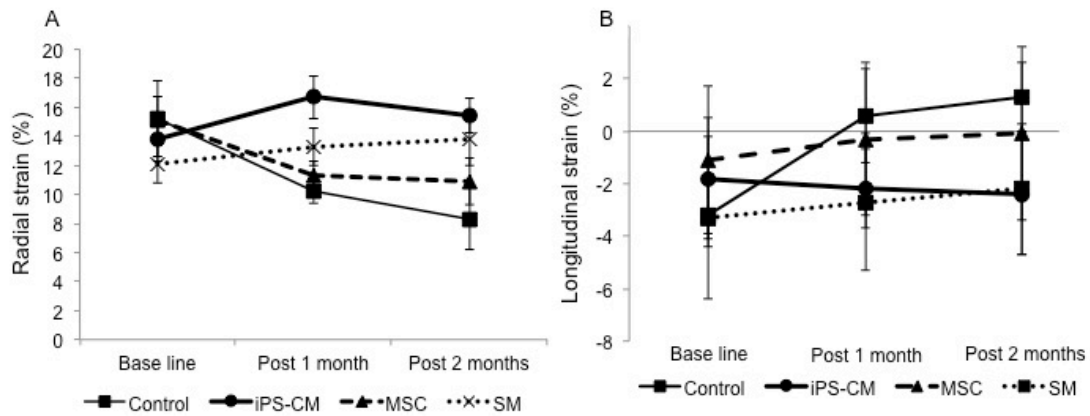


Figure S5. Quantitative assessment of myocardial wall stress in the RZ and BZ by the cardiac MRI. (A) Wall stress in the RZ. Regional wall stress was unchanged after treatment in this area. (B) Wall stress in the BZ. The iPS-CM therapy alleviated myocardial wall stress in the BZ when compared with that of the transplantation of other cell types and controls (*P < 0.05 vs. other groups; #P < 0.05 vs. baseline).

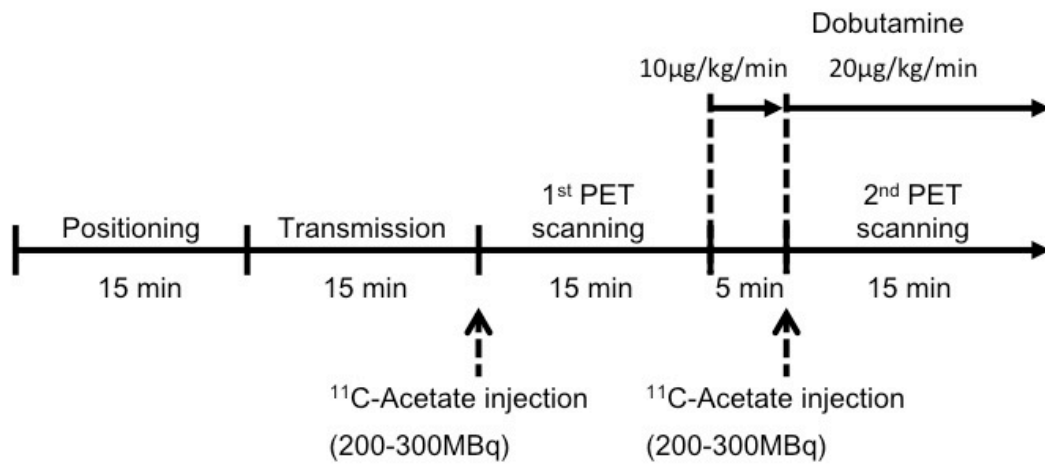


Figure S6. Regional cardiac function assessed by 2-D speckle tracking echocardiography. (A) Radial strain was evaluated from the mid-LV short-axis views. The mid-LV image was divided into six standard segments and time-strain curves were generated from each segment. The iPS-CM therapy had a higher effect on the radial strain than that of the other cell therapy groups; however, the difference was not statistically significant. (B) Longitudinal strain was assessed from the mid-levels in the long-axis views. The iPS-CM therapy caused higher radial strain than that of the other cell therapy groups; however, the difference was not statistically significant.

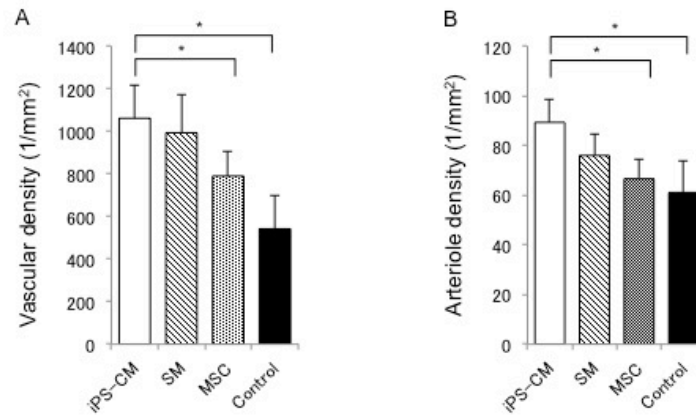


Figure S7. The iPS-CM therapy enhances vasculogenic response in the border zone (BZ). Vascular and arteriole densities were evaluated two months after cell therapy in the BZ sections of the hearts. (A) Vascular density was determined by counting the CD31+ vascular structures. (B) Arteriole density was determined by counting the vascular structures expressing both CD31 and SMA (*P < 0.05). Scale bar, 50 μ m.

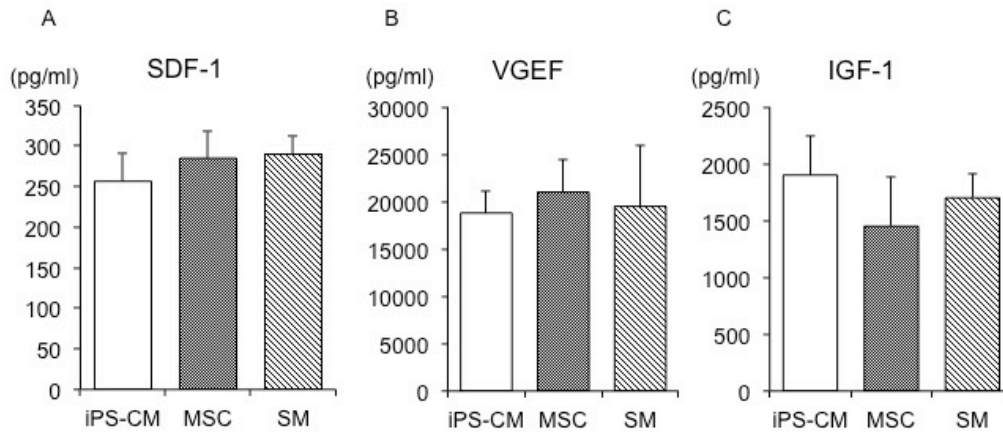


Figure S8. *In vitro* analysis of the cardiac protective factors by ELISA. The conditioned medium of the culture dishes in which 1×10^7 cells were seeded was collected to measure the concentration of SDF-1 (A), VEGF (B), and IGF-1 (C). There was no significant difference among the cell types.